SCIENTIFIC REPORTS

OPEN

SUBJECT AREAS:
HETEROGENEOUS CATALYSIS
STRUCTURAL PROPERTIES

Received
22 April 2014

Accepted
11 November 2014

Published
27 November 2014

Correspondence and requests for materials should be addressed to X.B.H. (huxb@nju.edu.cn) or Y.T.W. (ytwu@nju.edu.cn)

The Effect of Nano Confinement on the C–H Activation and its Corresponding Structure-Activity Relationship

Jing Shao, Linghua Yuan, Xingbang Hu, Youting Wu & Zhibing Zhang

School of Chemistry and Chemical Engineering, Nanjing University, Nanjing 210093, P. R. China.

The C–H activation of methane, ethane, and *t*-butane on inner and outer surfaces of nitrogen-doped carbon nanotube (NCNTs) are investigated using density functional theory. It includes NCNTs with different diameters, different N and O concentrations, and different types (armchair and zigzag). A universal structure-reactivity relationship is proposed to characterize the C–H activation occurring both on the inner and outer surfaces of the nano channel. The C–O bond distance, spin density and charge carried by active oxygen are found to be highly related to the C–H activation barriers. Based on these theoretical results, some useful strategies are suggested to guide the rational design of more effective catalysts by nano channel confinement.

Reactions or molecule structures confined in nano channels are quite different from those outside of channels. Such confinement effects widely exist in carbon nanotubes (CNTs), zeolites, and other mesoporous materials[1–6]. The confinement provides a potential method to control the reactivity of catalysts dramatically.

It was found from a variety of experiments that confinement effects could accelerate the reaction on the inner surface of channels[7–15], such as hydrogenation of CO to ethanol[7], Fischer-Tropsch chemistry[8], hydrolytic and kinetic resolution of epoxides[9], asymmetric hydrogenation[10], sulfoxidation[11], solvent-free esterifications[12], hydrogenation[13,14], photocatalytic reaction[15], and so on. Confinement can influence both the active phase and the reactants inside the CNTs. As a result, the reactions in channel are more effective[1,2,16].

Some experimental technologies (such as IR[17,18], in situ XRD[8], and neutron scattering[19]) have been successfully developed to investigate the chemical phenomena happening in nano channels. Because experimental measurements can only reflect an integration over multiple effects[20], theoretical calculations are still useful and important methods for understanding the origin of the structure and reaction inside the nano channels[21,22].

The confinement effects have been observed theoretically in many reaction processes, such as $D + H_2 \rightarrow HD + H$ in CNTs[23], ethylene oligomerization in zeolitic mesopores[24], propene metathesis reaction in zeolites[25], syngas reaction in CNTs[26], ethylene dimerization in zeolites[27], O_2 dissociation between two Pt (111)[28], H_2 dissociation in CNTs[29], and acetone tautomerization in zeolite[30]. Why does confinement influence the reaction in channels? Theoretical researches have revealed that confinement can change the interactions between reactant and catalyst[31–37]. Confinement can also influence the electronic structure of catalyst in channel[23–30]. In addition, confinement effect can even induce the variation of hydrophilic-hydrophobic property[38] and dynamical behavior[39] of the compounds in the nano channel.

It is believed that the reactions in the channel are influenced by the confinement whereas there is no such effect on the outer surface of channel[1–16,23–37]. It is important, though quite difficult, to describe the reaction both on the inner and outer surfaces of nano tube using the same model. If we can find a unified structure-reactivity relationship, it will build a bridge between reactions inside and outside of the nano tube.

Results

Modeling. The model used here is the C–H activation of methane by oxygen adsorbed on the inner and outer surfaces of nitrogen-doped carbon nanotubes (NCNTs). The model of NCNTs with adsorbed oxygen has been shown previously[40]. We also have discussed the adsorption and activation of oxygen on NCNTs[41,42], and the oxidation of methane on the surface of NCNTs by the adsorbed oxygen in previous papers[43]. In the oxidative dehydrogenation of ethane, the NCNT is also an effective catalyst[44]. The ability of these adsorbed oxygen in the

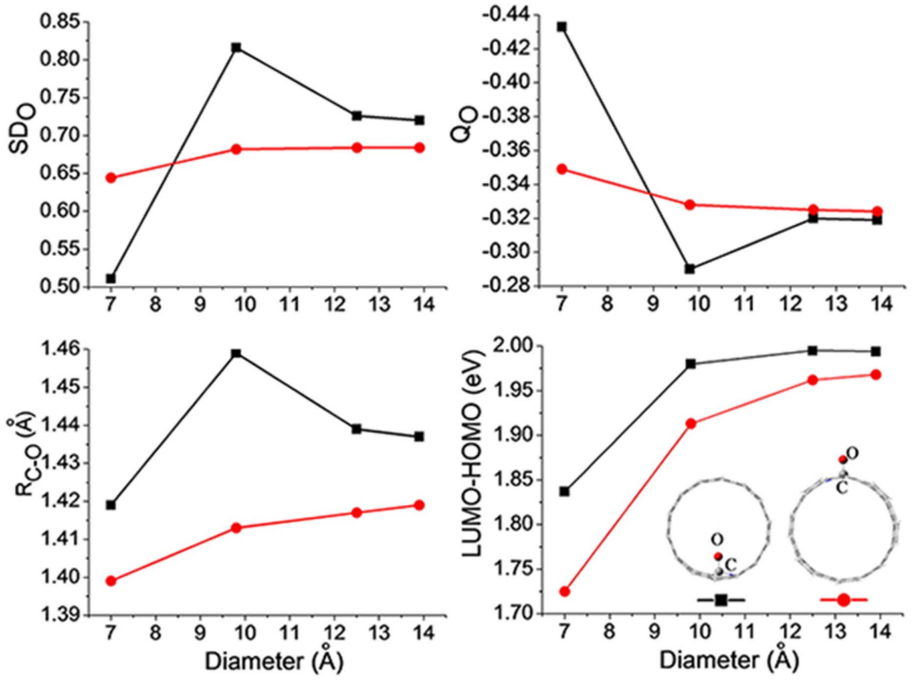

Figure 1 | The influences of NCNT diameter on the SD_O, Q_O, $R_{C\text{-}O}$, and LUMO-HOMO values with oxygen in (black square) and outside (red circle) of nano channel.

oxidation reactions have also been proved by experiments[45–47]. NCNTs used here are armchair nanotubes with delocalized σ electrons and terminated with C–H bonds, in which a nitrogen atom was placed substitutionally in the middle of a pure carbon nanotube[40]. The O atom is located on the surface of NCNTs with an optimized C–O bond length based on previous research of oxygen adsorption on NCNTs[40,41,43]. There are two ways to generate the active oxygen atom on the surface of NCNT: (1) O_2 dissociate on carbon atoms neighboring a nitrogen dopant of NCNT with a small dissociation barrier[48,49]. In this case, both of the oxygens are active[50]; (2) A hydrocarbon can be oxidized by the terminal oxygen of O_2 adsorbed on the surface of NCNT, and the remainder oxygen atom is active[43]. They are abbreviated as NCNT *(N, N)* (N = 5, 7, 9, and 10, the corresponding optimized diameters are 7.0, 9.8, 12.5, and 13.9 Å, respectively). For NCNT *(7, 7)*, different N concentrations are taken into consideration (0.82% and 2.45% for $C_{139}NH_{28}$ ($N_{0.82}$CNT *(7, 7)*) and $C_{137}N_3H_{28}$ ($N_{2.45}$CNT *(7, 7)*), respectively, see Supplementary information for the structure details). Correspondingly, NCNT with different O concentrations are investigated (0.93% and 2.72% for $C_{139}NOH_{28}$ and $C_{137}N_3O_3H_{28}$ respectively). The length of all NCNTs is 12.9 Å if not mentioned. Both reactions inside and outside of NCNT were taken into consideration. The following abbreviations are used: NCNT $(N,N)_{in}$-hydrocarbon or NCNT $(N,N)_{out}$-hydrocarbon means that the C–H activation of hydrocarbon is inside or outside of NCNT *(N, N)*, respectively.

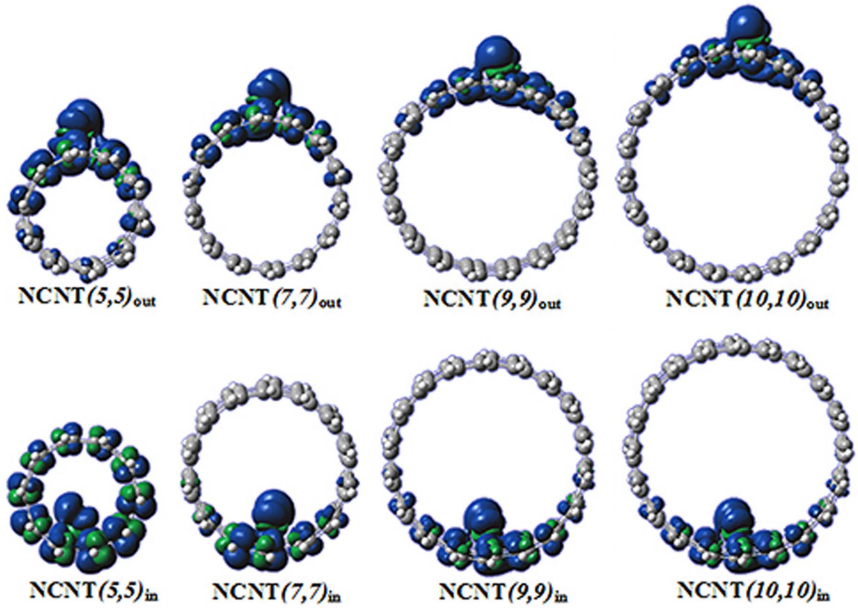

Figure 2 | The spin density distributions of NCNTs with active oxygen in and outside of the channel.

Table 1 | The C–H activation barrier ($E^{\neq}$) and substrate binding energy (BE) in or outside of different NCNTs[a]

	BE (in)	$E^{\neq}$ (in)	BE (out)	$E^{\neq}$ (out)
NCNT*(5,5)*–CH_4	32.2	66.4	−6.0	76.4
NCNT*(7,7)*–CH_4	−3.4	65.4	−6.6	74.2
NCNT*(7,7)*–C_2H_6	−2.8	46.4	−0.4	50.2
NCNT*(7,7)*–C_4H_{10}	5.0	34.4	−7.1	39.0
$N_{2.45}$CNT*(7,7)*–CH_4	−10.4	54.7	−7.0	73.6
NCNT*(9,9)*–CH_4	−5.2	70.3	−7.4	75.1
NCNT*(10,10)*–CH_4	−3.3	69.9	−4.9	74.0
NCNT*(11,0)*–CH_4	−9.4	125.6	-	-

[a]All energies are given in kJ/mol. 'In' means reaction in the channel and 'out' represents reaction outside of the channel.

Confinement effects on catalysts and C–H activation. First, the influences of confinement on the electronic and geometric characteristic of the adsorbed oxygen were investigated. Four parameters are taken into account, the spin density (SD_O) and charge (Q_O) carried by the active oxygen, the C–O bond length ($R_{C\text{-}O}$), and the gap between the lowest unoccupied and highest occupied molecular orbital (LUMO-HOMO) (Figure 1). It is obvious that the values in the inside of the NCNTs are quite different from those of outside, especially when the diameter of the channel is small. The SD_O, Q_O, $R_{C\text{-}O}$, and LUMO-HOMO gap obtained on outer surface of NCNTs show a monotonic increase or decrease with the increasing tube diameter. However, for the SD_O, Q_O, and $R_{C\text{-}O}$ values obtained inside NCNTs, there exists a inflection point for NCNT *(5, 5)* (diameter = 7.0 Å) that is induced by extreme confinement. To understand why the SD_O value of NCNT(5, 5)$_{in}$ is different from others, the spin density distributions of NCNTs with active oxygen inside and outside are presented in Figure 2. The spin density of NCNT(5, 5)$_{out}$, NCNT(7, 7)$_{in}$, NCNT(9, 9) and NCNT(10, 10) are mainly located around the active oxygen, whereas that of NCNT(5, 5)$_{in}$ is dispersed on the whole tube. As result, the SD_O value of NCNT(5, 5)$_{in}$ is far smaller than others.

When the diameter is larger than 7.0 Å, the curves become regular. The difference between the electronic and geometric parameters obtained inside or outside becomes smaller and smaller as the tube diameter increases, implying that the confinement effect becomes weaker and weaker. One can image that when the diameter of the tube is large enough, the inside and outside can be considered as two parallel sides of a plane. In this case, the confinement effect should disappear.

The oxidation of hydrocarbons includes two steps, C–H activation and C–O rebound[43,51–53]. The C–H activation is the rate-determining step in reactions catalyzed by NCNT[43] and other catalysts[51–53]. Herein, we focus on the C–H activation of methane, ethane, and *t*-butane on the inner or outer surfaces of NCNTs with different diameters. The imaginary frequencies of the transition state for the C–H activation are −1448.7, −1464.5, −1452.5 and −1442.8 in NCNT*(5,5)*$_{in}$–CH_4, NCNT*(5,5)*$_{out}$–CH_4, NCNT*(7,7)*$_{in}$–CH_4, and NCNT*(7,7)*$_{out}$–CH_4 respectively. These transition states have only one imaginary frequency and the values are big enough to show the corresponding structures are real transition states. The motion described by the eigenvector associated with these imaginary frequencies corresponds to the proton transfer from carbon to oxygen.

In all cases, the C–H activation barriers obtained inside are lower than those on the outside for the same substrate and NCNT (Table 1). Taking the reaction occuring on the inner and outer surface of NCNT*(7,7)* as example, B3LYP/6-31G structure optimization and energy calculation show that the methane C–H activation barrier obtained in channel is 8.8 kJ/mol lower than that obtained outside. A MP2/6-31G single point energy calculation shows that the barrier obtained inside is 26.1 kJ/mol lower than that obtained outside. Correspondingly, the H–C_{CH4} bond distances of the transition states obtained outside are larger than those obtained inside for the same NCNT (Figure 3). The order of the H–C_{CH4} bond distances is: NCNT*(5,5)*$_{in}$–CH_4 < NCNT*(7,7)*$_{in}$–CH_4 < NCNT*(9,9)*$_{in}$–CH_4 < NCNT*(10,10)*$_{in}$–CH_4 < NCNT*(5,5)*$_{out}$–CH_4 < NCNT*(7,7)*$_{out}$–CH_4

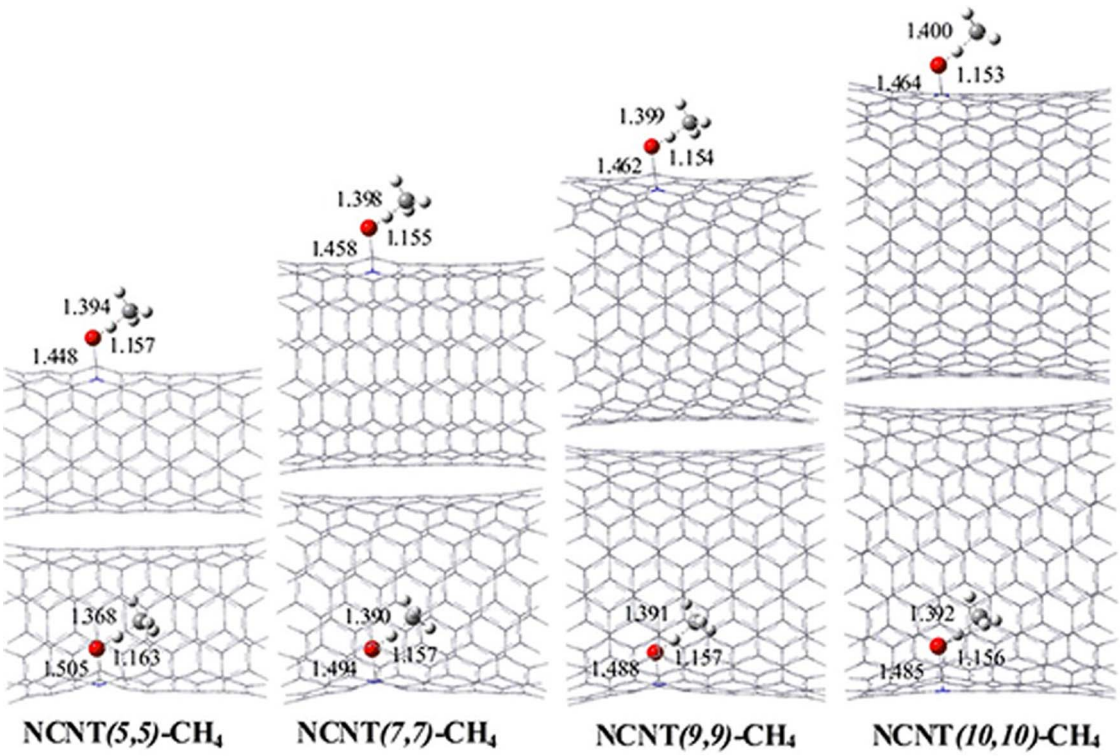

Figure 3 | The optimized transition states of methane C–H activation. The shown values are C_{NCNT}–O, O–H_{CH4} and H–C_{CH4} distances in Å.

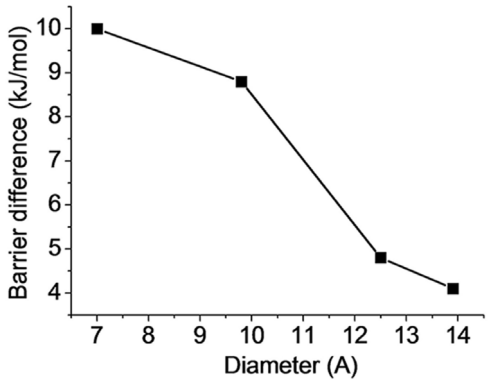

Figure 4 | The barrier difference of methane C–H activation in the inside and outside of the NCNT.

< NCNT*(9,9)*$_{out}$–CH_4 < NCNT*(10,10)*$_{out}$–CH_4. It suggests that confinement can shorten the proton transfer distance from reactant to transition states, which is beneficial for reducing the reaction barrier. Being consistent with the influence on electronic and structural parameters, a small diameter brings larger difference in C–H activation barrier (Figure 4). Even so, for the largest tube NCNT*(10,10)* investigated here, the energy difference of 4.1 kJ/mol will bring about 5 times enhancement of the reaction rate according to the transition state theory. These findings agree well with experimental results. Till now, most of the experiments have shown that the reactions performed in the inside of channel are faster than those of outside[7–15].

Previous researches using the model with only one N atom doping have revealed that the origin of catalytic activity of NCNTs is that the

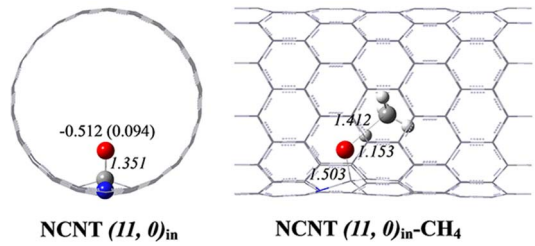

Figure 6 | The Q_O and SD_O values carried by zigzag NCNT*(11,0)* (left) and the optimized transition state (right). Values out and in parentheses are Q_O and SD_O values, respectively. The italic data are bond distances in Å.

N-doping can induce electron-deficient carbon around the doped N atom[40,41]. When three N atoms are doped in the nano tube, each N atom on the NCNT shows almost the same negative charge, and the carbon atoms around the nitrogen show similar positive charge comparing with the NCNT with only one N atom doping (Figure S1 in Supplementary information). It is interesting to find that each N–C part can be regarded as a new active center for the activation of oxygen. The O atom binding with any N–C part carries similar charge and spin density compared with the NCNT with only one N atom doping (Figure 5). As results, these O atoms are quite reactive for the C–H bond activation. The barriers of methane C–H activation on the inner and outer surface of $N_{2.45}$CNT *(7,7)* are 54.7 and 73.6 kJ/mol respectively. Though the barrier of C–H activation on different N–C part may have a little difference induced by the variation of SD_O and Q_O values in different region, these barrier heights are low enough to indicate the high reactivity of each N–C part. In this case, it is reasonable to believe that NCNTs doped with more N atoms will provide more active centers to adsorb and activate oxygen, which will

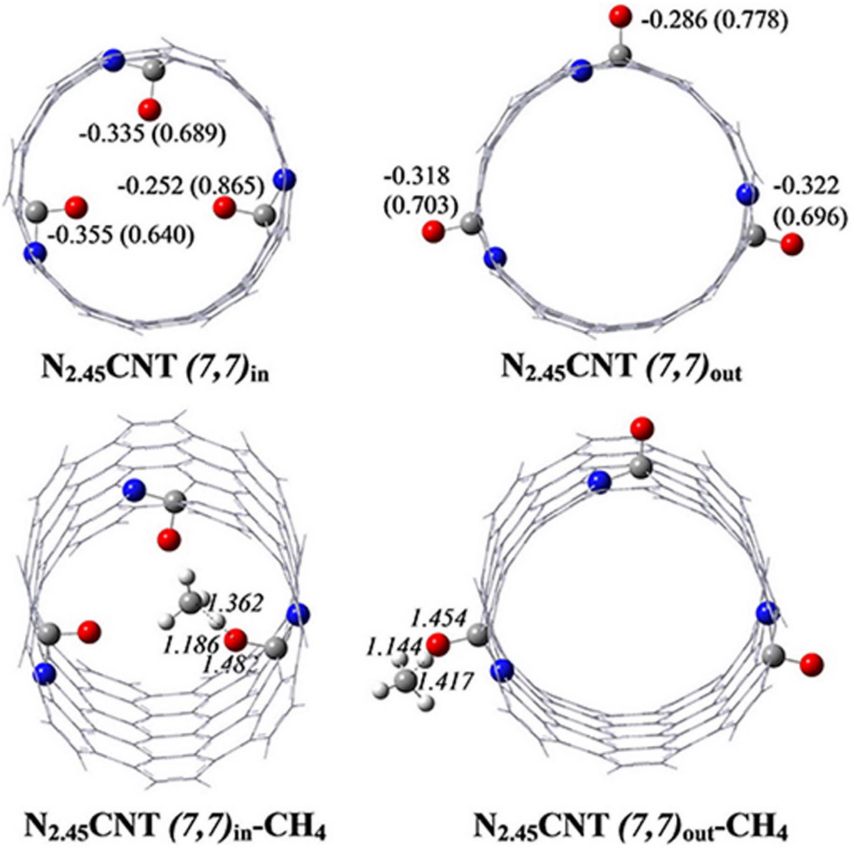

Figure 5 | The Q_O and SD_O values carried by $N_{2.45}$CNT*(7,7)* (upper) and the optimized transition state (lower). Values out and in parentheses are Q_O and SD_O values respectively. The italic data are bond distances in Å.

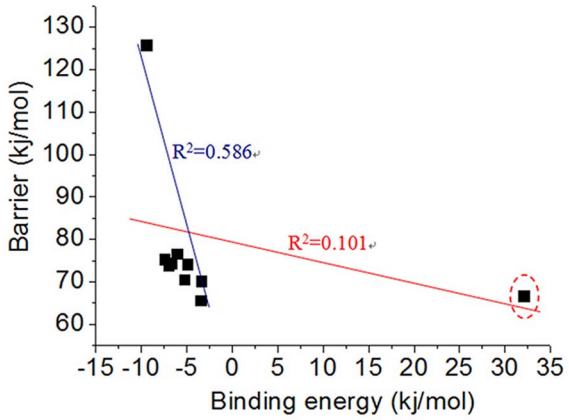

Figure 7 | The relationships between the reaction barrier and binding energy of methane.

make the NCNTs more powerful catalyst. In fact, experimental results have revealed that NCNT doped with 2.6% N atom is more active than that doped with 1.2% N atom[54].

Armchair and zigzag CNTs are two typical structures of nanotubes. A zigzag NCNT with diameter of 8.6 Å [NCNT *(11,0)*] was fully optimized and compared with the armchair NCNTs with similar diameter [NCNT *(7, 7)*] (Figure 6). It was found that the O atom in the inside of NCNT *(11,0)* is quite different from that of NCNT *(7, 7)*. The Q_O value of NCNT $(11,0)_{in}$ is more negative compared with all armchair NCNTs investigated here, and the SD_O value of NCNT $(11,0)_{in}$ is also smaller than those of all other armchair NCNTs. As a result, the methane C–H activation barrier obtained in the inside of NCNT *(11,0)* is quite high (125.5 kJ/mol).

Discussion

Structure-activity relationship. As we know, molecular structures and reactions occurring inside of the channel are influenced by confinement, whereas there has no such effect on the outer surface of channel[1–39]. It seems that it is quite difficult to describe the reaction in and outside of the channel by the same model. Does there exist a universal structure-reactivity relationship to predict the reactions occurring both inside and outside of channel?

The well-known BEP relations have revealed that the reactivity of catalysts is related to the binding strength of the reactant[55,56]. Herein, the C–H activation barrier is used as the y-axis to plot against the binding energy between methane and NCNTs in which only one oxygen binds with methane (Figure 7). If all structures are taken into consideration, there has no any relationship between reaction barrier and binding energy ($R^2 = 0.101$). It seems that the BEP relation does not work for NCNTs systems. The electronic and geometric parameters of NCNT$(5, 5)_{in}$ is abnormal due to the extreme confinement (Figure 1). The diameter of NCNT*(5, 5)* is so small (7.0 Å) that methane is hindered to enter the tube (Table 1). If the point belonging to NCNT$(5, 5)_{in}$ is not included in the data fitting, the correlation coefficient increases to 0.586. In this case, the activity of NCNTs are correlated with the binding energy of the reactant to some extent ($R^2 = 0.586$). Adsorption of reactant with small binding energy corresponds to low activation energy. This is similar to the case of ethylene hydrogenation on the surface of Pd/Au(111), Pd(111), Pd/Ru(0001) and Pd/Re(0001)[55]. For the nano confinement space, if the channel is too small, the adsorption of key reactant will be highly unfavorable. In this case, the reaction may be inhibited in confined space[57,58]. The activation of methane in NCNT*(5, 5)* and t-butyl in NCNT*(7, 7)* are two typical examples (Table 1).

To find out a more reasonable structure-activity relationship for nano confinement systems, the reaction barrier is used as the y-axis to plot against SD_O, Q_O, $R_{C\text{-}O}$ or LUMO-HOMO values, respectively (Figure 8). Similarly, the point belongs to NCNT$(5, 5)_{in}$ is not included in the data fitting due to the extreme confinement. It is interesting to note that SD_O, Q_O, and $R_{C\text{-}O}$ are highly related to the C–H activation barrier, no matter whether the reaction happens inside or outside of the surface. The correlation coefficients are 0.992, 0.990, and 0.846 for SD_O, Q_O, and $R_{C\text{-}O}$ respectively. Designing more powerful catalyst becomes much easier with these linear structure-reactivity relationships. Modification that leads to larger SD_O or $R_{C\text{-}O}$ will give a more powerful catalyst. According to the results presented in Figure 1, if the catalytic active center is inside of the channel, we should adopt small tube diameter to increase its reactivity. Indeed, this idea has been achieved in some experiments[1–6]. The challenges are how small the tube diameter can be

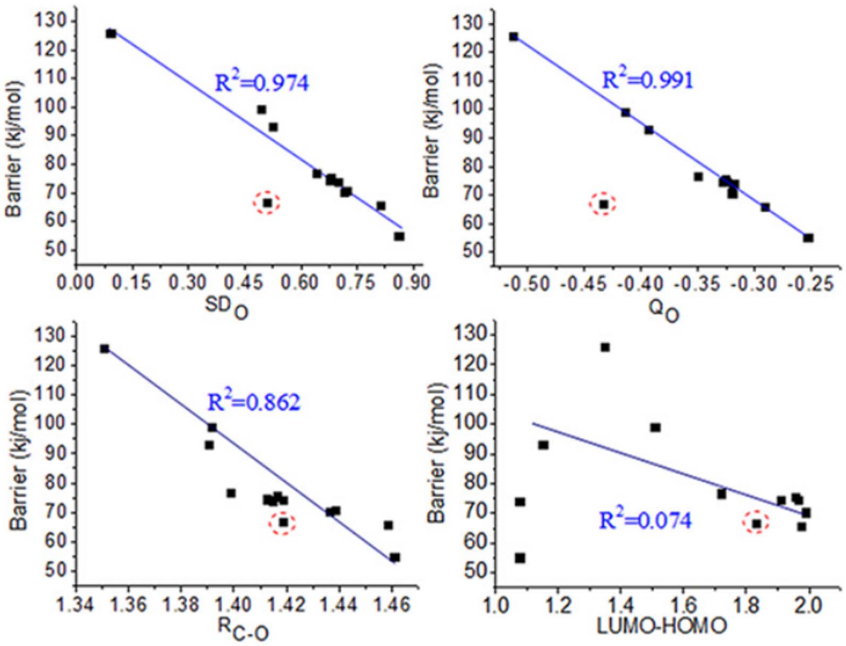

Figure 8 | The relationships between the reaction barrier and SD_O, Q_O, $R_{C\text{-}O}$ or LUMO-HOMO values.

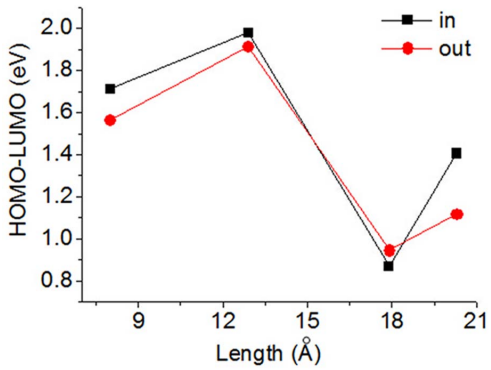

Figure 9 | The HOMO–LUMO gap of NCNTs with different tube length.

and whether the substrate can enter the tube smoothly when the tube is too small.

Though the HOMO-LUMO gap has been widely used to predict the reactivity of catalysts in homogeneous systems[59], it seems that this common method does not work in predicting the influence of confinement (Figure 8). There is no relationship between the LUMO-HOMO gap and reaction barrier obtained on the inner or outer surface of the channel. Though the electronic structure of O atom inside of zigzag NCNT is quite different from those of armchair NCNT, the structure-activity relationship revealed here can predict the C–H activation barrier on the surface of both armchair and zigzag NCNTs.

It should be noticed that the results obtained here are based on finite carbon nanotubes. Theoretical calculations that have adopted this method have achieved many successes in previous researches[27,28,37,40–43,53,60–67], including the prediction on the reactivity of NCNT[41,43] which has been proven by experiment[45–47]. Methods taking the periodic boundary condition into consideration may further improve these theoretical results. Though the influence of periodic boundary is not taken into consideration, theoretical researches using finite CNT and NCNT have revealed that the properties of carbon nanotubes exhibit a periodic behavior with increase in tube length[42,68,69]. For the systems investigated here, a periodic oscillation is also observed as the tube length increases (Figure 9). In order to investigate the influence of boundary, NCNT$(7, 7)_{out}$ with different lengths and terminals were calculated (Figure S2 in Supplementary information). Though the SD_O, Q_O and $R_{C\text{-}O}$ values of different NCNT$(7, 7)_{out}$ are various, their C–H activation barriers can be ascertained by the structure-activity relationship summarized in Figure 8.

In conclusion, based on a systematic DFT investigation on the C–H activation of methane, ethane, and *t*-butane on the inner and outer surface of NCNTs with different diameters, different N and O concentrations, and varying types (armchair and zigzag), the following can be stated: (1) The C–H activation processes investigated here perform more effectively inside of NCNTs due to the confinement effect. This effect is weakened as the tube diameter increases; (2) A universal structure-reactivity relationship was found for reactions occurring both on the inner and outer surface of nano channel. No matter whether the reactions occur inside or outside of the channel, SD_O, Q_O, or $R_{C\text{-}O}$ can be used to predict the C–H activation barrier. It gives a clear connection between reactions in and outside of nanotubes.

Methods

As a good compromise between computational efficiency and reasonable results, the density functional theory (DFT) based method is widely used for the calculation of nanotube[27,28,37,40–43,53,60–67] and small molecular activation using nanomaterial as catalysts[40–43,64]. Among these DFT based calculations, the B3LYP method is a good choice for nanotube and it has been shown to be in excellent agreement with the experimental data[27,37,40–43,47–52,60–65]. When B3LYP method is applied for NCNT systems, using different basis sets (6-31G, 6-311G, and aug-cc-pvdz) gave similar C–H activation barrier[43]. Hence, all the structures were optimized at the B3LYP/6-31G level of theory using the Gaussian 03 program.

The computed stationary points have been characterized as minima or transition states by diagonalizing the Hessian matrix and analyzing the vibrational normal modes. In this way, the stationary points can be classified as minima if no imaginary frequencies are shown or as transition states if only one imaginary frequency is obtained. The particular nature of the transition states has been determined by analyzing the motion described by the eigenvector associated with the imaginary frequency.

1. Pan, X. L. & Bao, X. H. The effects of confinement inside carbon nanotubes on catalysis. *Acc. Chem. Res.* **44**, 553–562 (2011).
2. Pan, X. L. & Bao, X. H. Reactions over catalysts confined in carbon nanotubes. *Chem. Commun.* **47**, 6271–6281 (2008).
3. Britz, D. A. & Khlobystov, A. N. Noncovalent interactions of molecules with single walled carbon nanotubes. *Chem. Soc. Rev.* **35**, 637–659 (2006).
4. Thomas, J. M. & Raja, R. Exploiting nanospace for asymmetric catalysis: confinement of immobilized, single-site chiral catalysts enhances enantioselectivity. *Acc. chem. Res.* **41**, 708–720 (2008).
5. Gounder, R. & Iglesia, E. The catalytic diversity of zeolites: confinement and solvation effects within voids of molecular dimensions. *Chem. Commun.* **49**, 3491–3509 (2013).
6. Goettmann, F. & Sanchez, C. How does confinement affect the catalytic activity of mesoporous materials? *J. Mater. Chem.* **17**, 24–30 (2007).
7. Pan, X. L. *et al.* Enhanced ethanol production inside carbon-nanotube reactors containing catalytic particles. *Nature mater.* **6**, 507–511 (2007).
8. Chen, W., Fan, Z., Pan, X. L. & Bao, X. H. Effect of confinement in carbon nanotubes on the activity of Fischer−Tropsch iron catalyst. *J. Am. Chem. Soc.* **130**, 9414–9419 (2008).
9. Yang, H., Zhang, L., Zhong, L., Yang, Q. & Li, C. Enhanced cooperative activation effect in the hydrolytic kinetic resolution of epoxides on [Co(salen)] catalysts confined in nanocages. *Angew. Chem. Int. Ed.* **46**, 6861–6865 (2007).
10. Chen, Z., Guan, Z., Li, M., Yang, Q. & Li, C. Enhancement of the performance of a platinum nanocatalyst confined within carbon nanotubes for asymmetric hydrogenation. *Angew. Chem. Int. Ed.* **50**, 4913–4917 (2011).
11. Liao, S., Coric, I., Wang, Q. & List, B. Activation of H_2O_2 by chiral confined Brønsted acids: a highly enantioselective catalytic sulfoxidation. *J. Am. Chem. Soc.* **134**, 10765–10768 (2012).
12. Karimi, B. & Vafaeezadeh, M. SBA-15-functionalized sulfonic acid confined acidic ionic liquid: a powerful and water-tolerant catalyst for solvent-free esterifications. *Chem. Commun.* **48**, 3327–3329 (2012).
13. Wang, D. *et al.* Confinement effect of carbon nanotubes: copper nanoparticles filled carbon nanotubes for hydrogenation of methyl acetate. *ACS Catal.* **2**, 1958–1966 (2012).
14. Castillejos, E. *et al.* Synthesis of platinum–ruthenium nanoparticles under supercritical CO_2 and their confinement in carbon nanotubes: Hydrogenation applications. *ChemCatChem* **4**, 118–122 (2012).
15. Li, T. *et al.* Confinement effect on Ag clusters in the channels of well-ordered mesoporous TiO_2 and their enhanced photocatalytic performance. *ChemCatChem* **5**, 1354–1358 (2013).
16. Castillejos, E. *et al.* An efficient strategy to drive nanoparticles into carbon nanotubes and the remarkable effect of confinement on their catalytic performance. *Angew. Chem. Int. Ed.* **48**, 2529–2533 (2009).
17. Byl, O. *et al.* Unusual hydrogen bonding in water-filled carbon nanotubes. *J. Am. Chem. Soc.* **128**, 12090–12097 (2006).
18. Hashimoto, S. *et al.* Anomaly of CH_4 molecular assembly confined in single-wall carbon nanohorn spaces. *J. Am. Chem. Soc.* **133**, 2022–2024 (2011).
19. Gallego, N. C., He, L., Saha, D., Contescu, C. I. & Melnichenko, Y. B. Hydrogen confinement in carbon nanopores: extreme densification at ambient temperature. *J. Am. Chem. Soc.* **133**, 13794–13797 (2011).
20. Santiso, E. E., Kostov, M. K., George, A. M., Nardelli, M. B. & Gubbins, K. E. Confinement effects on chemical reactions–Toward an integrated rational catalyst design. *Appl. Surf. Sci.* **253**, 5570–5579 (2007).
21. Turner, C. H., Brennan, J. K., Johnson, J. K. & Gubbins, K. E. Effect of confinement by porous materials on chemical reaction kinetics. *J. Chem. Phys.* **116**, 2138–2148 (2002).
22. Esteves, P. M. & Louis, B. Experimental and DFT study of the partial oxidation of benzene by N_2O over H-ZSM-5: Acid catalyzed mechanism. *J. Phys. Chem. B* **110**, 16793–16800 (2006).
23. Lu, T., Goldfield, E. M. & Gray, S. K. Classical trajectory studies of the D + H_2→ HD + H reaction confined in carbon nanotubes: Effects of collisions with the nanotube walls. *J. Phys. Chem. C* **114**, 9030–9040 (2010).
24. Toulhoat, H., Lontsi Fomena, M. & de Bruin, T. Computational study of the effect of confinement within microporous structures on the activity and selectivity of metallocene catalysts for ethylene oligomerization. *J. Am. Chem. Soc.* **133**, 2481–2491 (2011).
25. Jakobtorweihen, S., Hansen, N. & Keil, F. Combining reactive and configurational-bias Monte Carlo: Confinement influence on the propene metathesis reaction system in various zeolites. *J. Chem. Phys.* **125**, 224709 (2006).

26. Guan, J., Pan, X., Liu, X. & Bao, X. Syngas segregation induced by confinement in carbon nanotubes: a combined first-principles and Monte Carlo study. *J. Phys. Chem. C* **113**, 21687–21692 (2009).
27. Chu, Y., Han, B., Zheng, A. & Deng, F. Influence of acid strength and confinement effect on the ethylene dimerization reaction over solid acid catalysts: A theoretical calculation study. *J. Phys. Chem. C* **116**, 12687–12695 (2012).
28. Martínez de la Hoz, J. M. & Balbuena, P. B. Geometric and electronic confinement effects on catalysis. *J. Phys. Chem. C* **115**, 21324–21333 (2011).
29. Li, Z., Chen, Z.-X., Kang, G.-J. & He, X. Does confinement effect always enhance catalytic activity? A theoretical study of H_2 dissociation on CNT supported gold clusters. *Catal. Today* **165**, 25–31 (2011).
30. Boekfa, B., Pantu, P., Probst, M. & Limtrakul, J. Adsorption and tautomerization reaction of acetone on acidic zeolites: the confinement effect in different types of zeolites. *J. Phys. Chem. C* **114**, 15061–15067 (2010).
31. Habenicht, B. F. & Paddison, S. J. Ab initio simulations of the effects of nanoscale confinement on proton transfer in hydrophobic environments. *J. Phys. Chem. B* **115**, 10826–10835 (2011).
32. Hernandez-Rojas, J., Calvo, F., Bretón, J. & Gomez Llorente, J. Confinement effects on water clusters inside carbon nanotubes. *J. Phys. Chem. C* **116**, 17019–17028 (2012).
33. Gomez, D. A., Combariza, A. F. & Sastre, G. Confinement effects in the hydrogen adsorption on paddle wheel containing metal–organic frameworks. *Phys. Chem. Chem. Phys.* **14**, 2508–2517 (2012).
34. Rezouali, K., Belkhir, M. & Bai, J. Ab initio study of confinement and surface effects in AlN nanowires. *J. Phys. Chem. C* **114**, 11352–11357 (2010).
35. Wander, M. C. & Shuford, K. L. Molecular dynamics study of interfacial confinement effects of aqueous NaCl brines in nanoporous carbon. *J. Phys. Chem. C* **114**, 20539–20546 (2010).
36. De Toni, M., Pullumbi, P., Coudert, F.-X. & Fuchs, A. H. Understanding the effect of confinement on the liquid− gas transition: A study of adsorption isotherms in a family of metal− organic frameworks. *J. Phys. Chem. C* **114**, 21631–21637 (2010).
37. Kaczmarek-Kedziera, A. Confinement effect on p-nitroaniline electronic spectrum and electronic properties. *J. Phys. Chem. A* **115**, 5210–5220 (2011).
38. Yang, R., Hilder, T. A., Chung, S.-H. & Rendell, A. First-principles study of water confined in single-walled silicon carbide nanotubes. *J. Phys. Chem. C* **115**, 17255–17264 (2011).
39. Singh, R., Monk, J. & Hung, F. R. A computational study of the behavior of the ionic liquid $[BMIM^+][PF_6^-]$ confined inside multiwalled carbon nanotubes. *J. Phys. Chem. C* **114**, 15478–15485 (2010).
40. Gong, K., Du, F., Xia, Z., Durstock, M. & Dai, L. M. Nitrogen-Doped Carbon Nanotube Arrays with High Electrocatalytic Activity for Oxygen Reduction. *Science* **323**, 760–764 (2009).
41. Hu, X. B., Wu, Y. T., Li, H. R. & Zhang, Z. B. Adsorption and activation of O_2 on nitrogen-doped carbon nanotubes. *J. Phys. Chem. C* **114**, 9603–9607 (2010).
42. Hu, X. B., Liu, C., Wu, Y. T. & Zhang, Z. B. Density functional theory study on nitrogen-doped carbon nanotubes with and without oxygen adsorption: the influence of length and diameter. *New J. Chem.* **35**, 2601–2606 (2011).
43. Hu, X. B., Zhou, Z., Lin, Q., Wu, Y. T. & Zhang, Z. B. High reactivity of metal-free nitrogen-doped carbon nanotube for the C–H activation. *Chem. Phys. Lett.* **503**, 287–291 (2011).
44. Li, B. & Su, D. Theoretical studies on ethylene selectivity in the oxidative dehydrogenation reaction on undoped and doped nanostructured carbon catalysts. *Asian J. Chem.* **8**, 2605–2608 (2013).
45. Yu, H. *et al*. Selective catalysis of the aerobic oxidation of cyclohexane in the liquid phase by carbon nanotubes. *Angew. Chem. Int. Ed.* **50**, 3978–3982 (2011).
46. Chen, C. *et al*. Revealing the enhanced catalytic activity of nitrogen-doped carbon nanotubes for oxidative dehydrogenation of propane. *Chem. Commun.* **49**, 8151–8153 (2013).
47. Sun, X. J. *et al*. A class of high performance metal-free oxygen reduction electrocatalysts based on cheap carbon blacks. *Sci. Rep.* **3**, 2505 (2013).
48. Shan, B. & Cho, K. Oxygen dissociation on nitrogen-doped single wall nanotube: A first-principles study. *Chem. Phys. Lett.* **492**, 131–136 (2010).
49. Ni, S., Li, Z. Y. & Yang, J. L. Oxygen molecule dissociation on carbon nanostructures with different types of nitrogen doping. *Nanoscale* **4**, 1184–1189 (2012).
50. Hu, X. B., Wu, Y. T. & Zhang, Z. B. CO oxidation on metal-free nitrogen-doped carbon nanotubes and the related structure–reactivity relationships. *J. Mater. Chem.* **22**, 15198–15205 (2012).
51. de Visser, S. P., Kumar, D., Cohen, S., Shacham, R. & Shaik, S. A predictive pattern of computed barriers for CH hydroxylation by compound I of cytochrome P450. *J. Am. Chem. Soc.* **126**, 8362–8363 (2004).
52. Hu, X. B., Sun, Y., Mao, J. Y. & Li, H. R. Theoretical study on the structure–reactivity relationships of acetylacetone–Fe catalyst modified by ionic compound in C–H activation reaction. *J. Catal.* **272**, 320–332 (2010).
53. Hu, X. B. & Li, H. R. All-metal aromatic complexes show high reactivity in the oxidation reaction of methane and some hydrocarbons. *J. Phys. Chem. A* **111**, 8352–8356 (2007).
54. Chizari, K. *et al*. Nitrogen-doped carbon nanotubes as a highly active metal-free catalyst for selective oxidation. *ChemSusChem* **5**, 102–108 (2012).
55. Pallassana, V. & Neurock, M. Electronic factors governing ethylene hydrogenation and dehydrogenation activity of pseudomorphic PdML/Re(0001), PdML/Ru(0001), Pd(111), and PdML/Au(111) Surfaces. *J. Catal.* **191**, 301–317 (2000).
56. van Santen, R. A., Neurock, M. & Shetty, S. G. Reactivity theory of transition-metal surfaces: A bronsted-evans-polanyi linear activation energy-free-energy analysis. *Chem. Rev.* **110**, 2005–2048 (2010).
57. Xiong, H. F., Zhang, Y. H., Wang, S. G., Liew, K. Y. & Li, J. J. Preparation and catalytic activity for fischer-tropsch synthesis of ru nanoparticles confined in the channels of mesoporous SBA-15. *J. Phys. Chem. C* **112**, 9706–9709 (2008).
58. Zheng, W. Q. *et al*. Structure-function correlations for Ru/CNT in the catalytic decomposition of ammonia. *ChemSusChem* **3**, 226–230 (2010).
59. Rss, D. H. & Houk, K. N. Theory of 1,3-Dipolar Cycloadditions: Distortion/ Interaction and Frontier Molecular Orbital Models. *J. Am. Chem. Soc.* **130**, 10187–10198 (2008).
60. Chen, Z. *et al*. Side-wall opening of single-walled carbon nanotubes (SWCNTs) by chemical modification: A critical theoretical study. *Angew. Chem. Int. Ed.* **43**, 1552–1554 (2004).
61. Lu, X., Chen, Z. & Schleyer, P. v. R. Are stone-wales defect sites always more reactive than perfect sites in the sidewalls of single-wall carbon nanotubes? *J. Am. Chem. Soc.* **127**, 20–21 (2005).
62. Zheng, G., Wang, Z., Irle, S. & Morokuma, K. Origin of the linear relationship between CH/NH/O-SWNT reaction energies and sidewall curvature: Armchair nanotubes. *J. Am. Chem. Soc.* **128**, 15117–15126 (2006).
63. Nikawa, H. *et al*. Missing metallofullerene with C_{80} cage. *J. Am. Chem. Soc.* **131**, 10950–10954 (2009).
64. Gao, X. *et al*. Oxidation unzipping of stable nanographenes into joint spin-rich fragments. *J. Am. Chem. Soc.* **131**, 9663–9669 (2009).
65. Li, J., Zhou, G., Chen, Y., Gu, B. & Duan, W. Magnetism of C adatoms on BN nanostructures: Implications for functional nanodevices. *J. Am. Chem. Soc.* **131**, 1796–1801 (2009).
66. Xiao, J. *et al*. Theoretical prediction of electronic structure and carrier mobility in single-walled MoS_2 nanotubes. *Sci. Rep.* **4**, 4327 (2014).
67. Zhang, P., Xiao, B. B., Hou, X. L., Zhu, Y. F. & Jiang, Q. Layered SiC sheets: A potential catalyst for oxygen reduction reaction. *Sci. Rep.* **4**, 3821 (2014).
68. Zurek, E. & Autschbach, J. Density Functional Calculations of the 13C NMR Chemical Shifts in (9,0) Single-Walled Carbon Nanotubes. *J. Am. Chem. Soc.* **126**, 13079–13088 (2004).
69. Bettinger, H. F. Effects of finite carbon nanotube length on sidewall addition of fluorine atom and methylene. *Org. Lett.* **6**, 731 (2004).

Acknowledgments

This work was supported by the National Natural Science Foundation of China (No. 21176110 and 21376115) and Jiangsu Province Natural Science Foundation (BK20141311). Thanks to Liu Liu and Cory Weinstein in the University of California San Diego for discussion.

Author contributions

X.B.H. and Y.T.W. proposed the idea, analyzed the data and wrote the paper. J.S. and L.H.Y. performed the calculations. Z.B.Z. participated in the discussion and revised the manuscript. All authors reviewed the manuscript.

Additional information

Supplementary information accompanies this paper at http://www.nature.com/scientificreports

Competing financial interests: The authors declare no competing financial interests.

How to cite this article: Shao, J., Yuan, L., Hu, X., Wu, Y. & Zhang, Z. The Effect of Nano Confinement on the C–H Activation and its Corresponding Structure-Activity Relationship. *Sci. Rep.* **4**, 7225; DOI:10.1038/srep07225 (2014).